LBL-29994

Center for Advanced Materials

CAM

A Study of the Influence of Temperature Gradients on Densification of Glass Powder Compacts

R.B. Cinque
(M.S. Thesis)

December 1990

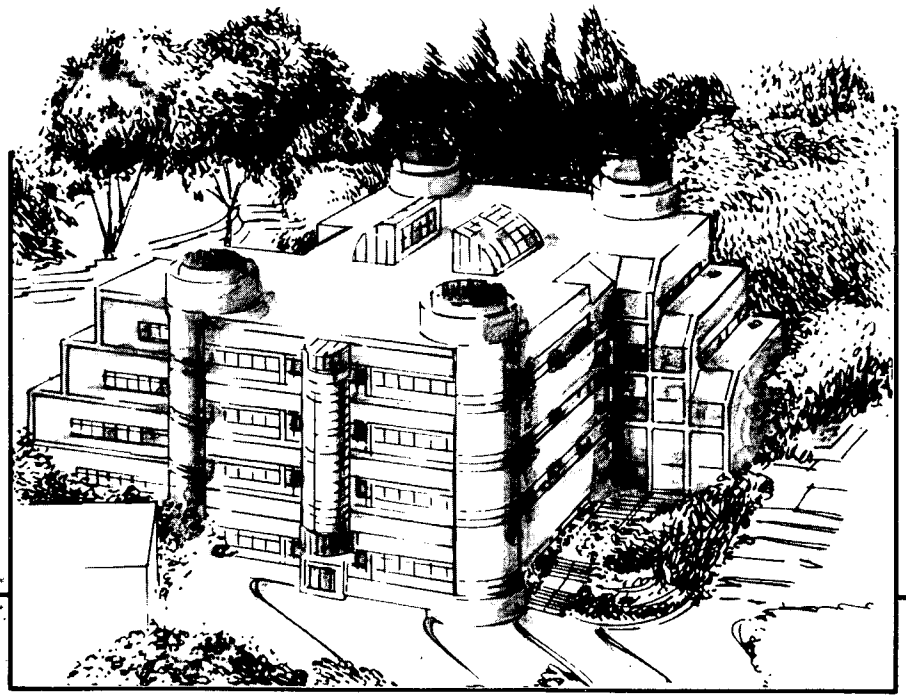

Materials and Chemical Sciences Division

Lawrence Berkeley Laboratory • University of California

ONE CYCLOTRON ROAD, BERKELEY, CA 94720 • (415) 486-4755

Prepared for the U.S. Department of Energy under Contract DE-AC03-76SF00098

LOAN COPY
Circulates
for 4 weeks
Bldg. 50 Library.
LBL-29994
Copy 2

DISCLAIMER

This document was prepared as an account of work sponsored by the United States Government. While this document is believed to contain correct information, neither the United States Government nor any agency thereof, nor the Regents of the University of California, nor any of their employees, makes any warranty, express or implied, or assumes any legal responsibility for the accuracy, completeness, or usefulness of any information, apparatus, product, or process disclosed, or represents that its use would not infringe privately owned rights. Reference herein to any specific commercial product, process, or service by its trade name, trademark, manufacturer, or otherwise, does not necessarily constitute or imply its endorsement, recommendation, or favoring by the United States Government or any agency thereof, or the Regents of the University of California. The views and opinions of authors expressed herein do not necessarily state or reflect those of the United States Government or any agency thereof or the Regents of the University of California.

LBL-29994

A Study of the Influence of Temperature Gradients on Densification of Glass Powder Compacts

Russell B. Cinque

M. S. Thesis

Department of Materials Science and Mineral Engineering
University of California

and

Center for Advanced Materials
Materials Sciences Division
Lawerence Berkeley Laboratory
University of California
Berkeley Ca 94702

December 12, 1990

This work is supported by the Director, Office of Energy Research, Office of Basic Energy Science, Material Sciences Division of the U.S. Department of Energy under Contract No. DE-AC03-76SF00098

Table of Contents

1 INTRODUCTION 1

2 THEORY 8

3 EXPERIMENTAL PROCEDURE 10
3.1 Powder Characterization 10
3.2 Sample Preparation 12
3.3 Sintering 13
3.4 Chemical Segregation 16

4 DISCUSSION 17
4.1 Density Measurement 17
4.2 Chemical Segregation 20

5 CONCLUSION 22

6 TABLES 23

7 FIGURES 29

Table of Figures

Starting Material 29
X-ray pattern of starting material 30
X-ray diffraction pattern of heated material 31
Classified Material 32
Classified Material 33
X-ray pattern of starting material 34
X-ray diffraction pattern of heated material 35
X-ray pattern of starting material 36
X-ray diffraction pattern of heated material 37
SEM Micrographs of Isothermal Samples 38
SEM Micrographs of Gradient Samples 39
X-ray diffraction pattern of heated material 40

Table of Tables

Isothermal Density Measurements 23
Gradient Density Measurements 24
Glass Composition 26
Isothermal Composition Profile 27
Gradient Compostition Profile 28

1 INTRODUCTION

Most commercial ceramics are produced by sintering, which is the name given to the complex set of changes grain size and shape, in pore shape, and in pore size and distribution which are produced by firing porous powder compacts at temperatures below the melting point. Usually, the desired product of sintering is a fully dense solid of small grain size. The desired mechanical and optical properties of sintered solids often are strongly dependent on density and microstructure. Consequently, many ceramists have focused research efforts on understanding the sintering process, and in particular how sintering produces densification.

The accepted driving force for densification is the reduction of surface free energy[1]. Surface free energy is reduced by eliminating solid-vapor interfaces and replacing them with lower energy solid-solid interfaces. Reduction of surface energy can be achieved by transporting matter from either the surface or bulk and depositing it at the neck regions between particles. When matter is transported from within the bulk particle, the centers approach and the system densifies.

Let us consider the general outline of densification in powder compacts. The unfired powder compacts, referred to as green bodies, initially range in porosity anywhere from 25 to 70% by volume, depending on the material and processing. The pores of such compacts form a continuous interconnecting network of channels. To produce the desired increase in density, the green bodies are held at elevated temperatures. During the initial stages of heating, material is transported to the regions of contact between particles, forming necks. Since the solid-vapor surface area of green bodies is large, there is a large driving force for mass transport and the initial rate of

transport is high. As sintering proceeds, the necks between particles grow, reducing the solid-vapor surface area and thus reducing the driving force for further densification. Eventually neck growth causes the pores to become isolated. The final stages of sintering are characterized by relatively slow densification which is achieved by pore rounding and elimination. Thus, the rate of sintering is dependant on the constantly changing morphology of the compact.

The rate at which sintering proceeds is dependent not only on the morphology of the sample, but also upon the mechanism of transport. For glass, which is the material used in the present study, the mechanism of transport is viscous flow. The initial rate of sintering by viscous flow was derived by Frenkel[2]. He argues that crystalline solids can deform by vacancy diffusion processes that cause deformations like those characteristic of viscous flow. His model starts with two viscous spheres originally in contact at a single point. The spheres approach, producing a circular area of contact. By equating the energy dissipated through viscous flow with that gained by reducing surface area, he produced equation (1) which gives the predicted area of contact after a period of coalescence.

$$x^2 = \frac{3}{2}\frac{a\gamma}{\eta}t \tag{1}$$

x = contact diameter

a = particle radius

γ = surface tension

t = time

η = viscosity

The general form of this relationship was experimentally confirmed by many investigators. Kucznski[3] examined the early stages of sintering by measuring the area of contact between glass spheres and a glass plate as a function of time. Experiments were done in air at various temperatures. At each temperature Kuczynski found a linear relation between contact area and time. He concluded that the glass sintered viscously at the rate predicted by Frenkel's equation. This conclusion was supported by Kingery and Berg[4] who also preformed experiments in which the areas of contact between paired glass spheres were measured as a function of time. Subsequent investigators expanded Frenkel's theory to include models of final stage sintering as well as alternate models of the initial stage. Mackenzie and Shuttleworth[5] used an energy balance to calculate the rate of closure of isolated pores. Zaplatynski[6] provided experimental support by measuring the rate of closure of thick walled capillary tubes.

In recent years, investigators have noted anomalies in the rates of sintering of crystalline ceramics. Unusually high densities are produced by fast firing, that is by raising the temperature rapidly and then cooling without a significant time of isothermal heating [7,8]. Fast firing differs significantly from the firing used in conventional sintering in that both the rate of heating and the resulting temperature gradients in fast firing are much larger. When temperature gradients are present, accepted sintering theory models any gradient as a series of isothermal zones, so that each segment of the compact sinters at a rate governed by the local temperature. Thus, temperature gradients are implicitly predicted not to provide a driving force for densification. As a result, research has focused on understanding how the rate of heating effects densification.

Cutler[9] studied the initial rate of sintering of glass compacts at constant heating rates. The compacts were made with a spherical soda-lime glass powder that ranged from 15 to 25 microns in diameter. Sintering was done in a controlled atmosphere of

oxygen saturated with water vapor using rates of 0.46 to 2.91 $^{o}C/min$. Cutler compared his results to a simple extension of Frenkel's isothermal model which assumed that each segment of the compact would sinter at a rate governed by the local temperature, and he approximated viscosity as a thermally activated process with a temperature independent activation energy. Cutler found good agreement between his model and the experimental data. Harmer and Brook[7] have shown that rapid heating rates, which they termed fast firing, caused Al_2O_3 to densify with less grain growth than observed in more conventional firing cycles. They suggested a simple explanation, that the activation energy for densification is greater than that for grain growth.

More recently, Chu et al.[10] studied the effects of constant heating rates on compacts of ZnO. Using a relatively wide range of heating rates (0.5 to 15 $^{o}C/min$) they found that at low temperature the densification rate as a function of temperature increased almost linearly with heating rate. However, the incremental densification achieved was dependent on the degree of coarsening. Thus, coarsening, defined by the increase in pore spacing, was of central importance. They conclude that when there is significant coarsening the density at a given temperature may be independent of heating rate, while in cases with little or no coarsening, the incremental densification is an inverse function of heating rate.

The models derived by Cutler and by Chu et al. describe sintering during temperature change as a sequence of isothermal processes. That is, sintering proceeds at a rate governed by the local temperature. When heating causes the local temperature to increase the local sintering rate also increases. Since faster heating rates produce a more rapid increase in temperature they also produce a more rapid increase in the rate of sintering. However, since less time is spent at a given temperature, the incremental

densification may be less. These models do not predict increased densification as a result of rapid heating, thus this line of analysis implies that the high density produced by fast firing must be caused by time spent at the very high temperature.

Ivensen[11] found results that could not be explained by such "isothermal" extensions of sintering theory. In his first set of experiments he investigated the effect of heating rate on the shrinkage of nickel powder compacts. He found the rates of shrinkage were much increased over the rates expected from measurements at constant temperature during the ramp and decreased as the isothermal temperature was approached. The fact that the rate of shrinkage sharply decreased while the temperature of the compact continued to increase is of great significance. If his observations are not subject to an unidentified error, the rate of sintering was somehow dependent on the rate of heating. Ivensen first thought that the high initial rates reflect a high concentration of defects present before heating was begun. However, he performed a second set of experiments which showed that this explanation could not be correct. By using a series of ramps and isothermal soaks, he showed that the rapid shrinkage must be due to the state of the powder during the ramp, which is directly related to the rate of temperature increase. Ivensen went on to speculate that the unusually high densification rate could be explained by the creation of active defects during heating and their subsequent annihilation.

Another possible explanation for Ivensen's results may be that temperature gradients increase the densification rate. Heating always involves transient temperature gradients, and all materials will experience an internal temperature gradient during heating. The magnitude and duration of the gradient will depend upon the rate of heating and the thermal conductivity of the material and its surroundings. If temperature gradients provide a driving force for mass transport, they could cause the transient increase in the rate of shrinkage that Ivensen observed. Temperature gradients could

then also be responsible for the increased densification produced by fast firing. Since fast firing differs from conventional heating schedules by using a steep ramp to a relatively hot, short soak, large temperature gradients are inherent in the process. These large gradients could accentuate an effect that had gone undetected in samples that were fired with a conventional heating schedule. If temperature gradients were responsible for enhanced densification during increases in sample temperature, it should be possible to obtain similar, but larger effects in static temperature gradients, which would provide a continuous driving force for enhanced densification.

Evidence to support the belief that static temperature gradients do increase the rate of sintering was provided by Braudeau, et al[12]. A series of channels were lithographically introduced into a single crystal of alumina. Heating the samples in air at temperatures of 1600°C caused decay in the amplitudes of the channels. Decay was measured for samples heated isothermally and in temperature gradients of 60°C/cm. Samples heated in gradients showed more rapid decay than comparable isothermal samples. Braudeau, et al. believe that temperature gradients were responsible for increased mass transport and that gradients may explain the rapid sintering observed when ceramics are fast fired.

The evidence that gradients drive mass transport through liquids or vapor, coupled with evidence that surface diffusion on solids and vapor transport are closely related processes, led Searcy to predict that gradients could also enhance densification during sintering[13,14]. This theory was confirmed by Beruto et al.[15,16] who preformed a series of studies on the densification of MgO pellets. Because the sintering of MgO is catalyzed by water vapor, complications produced by the presence of thermal gradients during heating and cooling could be avoided. Significant sintering began only when water vapor was introduced after a sample reached constant isothermal conditions or after it had

attained a prescribed temperature gradient. Also, since MgO is a pseudo one-component phase, there were no problems with chemical de-mixing. In the first set of experiments, pellets were sintered both isothermally and in static temperature gradients of about 100°C/cm. Beruto found that the pellets sintered in gradients were more dense at each local temperature in the gradient than was predicted by modeling the gradient as a series of isothermal zones. With Ivensen's work as a reference, a second series of experiments were preformed. MgO pellets were thermally cycled to study the importance of the rate of temperature change. The authors found no significant effect on densification and concluded that the temperature gradient, rather than the rate of change was responsible for observed increases in densification.

In the present study, we are concerned with the influence of temperature gradients on densification during the early stages of sintering in glass powder compacts. Glass was chosen primarily because it is of interest to determine if gradients can enhance densification, not only by diffusion in crystalline particles, as was observed with MgO, but also by viscous flow. A second reason for using glass was that glasses clearly have the isotropic surface energies assumed in sintering models. The assumption that surface energies are isotropic is not always valid for crystalline ceramics and that assumption has been shown to lead to predictions for grain growth which are in conflict with observations. Furthermore, grain boundary free energies, which are often neglected in sintering models, are absent when glass is sintered. The models of isothermal sintering derived from Frenkel's work have been quite successful in describing much experimental data. However, the work of Ivensen, Bradeau, and Beruto suggest a need for sintering studies which evaluate the influences of temperature gradients.

2 THEORY

As noted previously, the driving force for densification is the reduction in surface and interfacial free energies. In high temperature solids surface energies are usually assumed to be isotropic. With this approximation, changes in surface free energies become directly proportional to changes in surface areas. Surface areas are reduced when matter is transferred from regions of low positive curvature to regions of lower positive or of negative curvature. In a powder compact, transfer of matter to the area of contact between particles reduces the surface area and, therefore, lowers the total surface energy of the compact. If the transfer is from a grain boundary or from within the particles in contact at a neck, densification results.

When the sample is isothermal, and the surface energies are isotropic, the driving force for diffusion is given by the Kelvin equation, which relates the curvature to the difference in vapor pressure.

$$RT\ln\left(\frac{p_1}{p_2}\right)=\gamma\Omega(K_1-K_2) \tag{2}$$

p_1, p_2 = vapor pressure

γ = surface energy

Ω = atomic volume

K_1, K_2 = surface curvature

This equation shows that as particle size increases the driving force for diffusion will decrease. Note that while rates of diffusion are mechanism dependent, the driving

force is not. Thus, equation (2) is applicable to any system in which curved surfaces are present.

Temperature gradients provide an additional driving force for mass transport and, therefore at least potentially for densification. The driving force for vapor phase transport of a one-component or pseudo one-component solid or a liquid of negligible surface area in terms of its vapor pressure variation with temperature is given by equation (3)

$$RT\ln\frac{p_1^0}{p_2^0}=\left(\frac{\Delta G_1^0}{RT_1}\right)-\left(\frac{\Delta G_2^0}{RT_2}\right) \tag{3}$$

p_1^0, p_2^0= equilibrium vapor pressures at T_1 and T_2

$\Delta G_1^0, \Delta G_2^0$= the standard free energies of vaporization

Searcy suggests that just as the Kelvin equation, eq. (2), describes the driving force for isothermal sintering by any diffusional process, eq. (3) describes an additional driving force provided by temperature gradients for mass transport and for sintering by any diffusional path. If so, the driving force in a gradient can be obtained by adding eqs. (2) and (3).

$$RT\ln\frac{p_1 p_1^0}{p_2 p_2^0}=\gamma\Omega(K_1-K_2)+\left(\frac{\Delta G_1^0}{RT_1}\right)-\left(\frac{\Delta G_2^0}{RT_2}\right) \tag{4}$$

To test this model, in the present work we attempt to isolate the possible effects of gradients on sintering by viscous flow. An important secondary goal is to determine if significant chemical segregation occurs during the heating of the glass.

3 EXPERIMENTAL PROCEDURE

3.1 Powder Characterization

Sample pellets are prepared from a sodium silicate glass obtained from the Jaygo corporation. The particles (shown in figure 1) are, with few exceptions, solid spheres which range in size from 15 to 100 μm. The manufacturer's reported composition is given in the first row of table 4. This table also contains measurements of composition that were made by energy dispersive X-ray analysis (EDX) in a scanning electron microscope. The detector, equipped with a thin window, does not give quantitative measurements for boron, but was able to detect the other constituents reported by the manufacturer. The starting powder was mounted using carbon paste and then was flash coated with a layer of carbon to provide conduction. EDX data were collected in three separate runs with the electron beam focused on a single particle. The single particle provided a relatively flat surface which minimized the variation of take off angle. The results of these measurements are show in rows 2-4 of table 4. Measured elemental weight percentages were converted to compound weight percentages. The average and standard deviation is calculated for each component. As a measure of the reliability, we calculate the ratio of the standard deviation to the average.

Measured quantities are lower for the light elements and greater for the heavy elements than reported in the manufacturer's specifications. This discrepancy is not important for our study since we are not investigating the effects of composition. The

important question is whether compositions change or become non-uniform during heating. These issues are important because the theory that predicts increased densification has been developed only for condensed phases of constant composition.

To support the supposition that viscous flow was the dominant mechanism of transport in this glass, it was necessary to ensure that significant loss of volatile components of the glass did not occur during sintering. A weight loss experiment was performed by placing a thin layer of powder on platinum foil and heating for 24 hours at 700 ^{o}C. Less than 0.05% of the powder was lost during this time. It was also necessary to determine whether the originally amorphous powder remained amorphous during sintering. Figure 2 shows the X-ray diffraction pattern for the starting material. Figure 3 shows the pattern for a sample that was heated for 24 hours at 700°C then ground to pass through a #200 mesh screen. These patterns clearly show that the glass has not crystallized. We conclude that vaporization and crystallization are negligible in the time of our sintering runs and that viscous flow will be the dominant mechanism of sintering.

Before pressing, the powder was classified with sieves. To minimize the driving force of surface curvature relative to that from a temperature gradient it is desirable to use powder particles of relatively large cross section. However, as powder size increased, the mechanical stability of the pellets decreased. Stable pellets were produced using the powder collected between # 200 and # 325 mesh screens. This classification produced a slightly more uniform powder, with particles ranging in size from 30μm-100μm. The classified powder is shown in figure 4. The powder density was measured using the Archemedie's displacement principle. This measurement confirmed the manufactuer's reported value of 2.55 g/cm^3.

3.2 Sample Preparation

Sample pellets 0.85 cm in diameter and approximately 1.2 cm in length were produced by means of a syringe extrusion technique similar to that used by Beruto et al.[16]. First powder and water were mixed in the syringe. The slurry was then stirred to remove bubbles. Pressing against absorbent paper removed excess liquid and compacted the wet powder. The mixture was extruded and trimmed. An indentation about 1 mm in diameter and 1 mm deep was made in each end of the pellet. The indentations provided holds for thermocouples which in turn provide support for the pellets during sintering. The damp pellets were placed on platinum foil and oven dried at 60°C overnight.

At this point the pellets were mechanically fragile, making them difficult to handle. To overcome this problem the pellets were pre-sintered. The platinum foil which supported the pellets was placed on an alumina boat. The boat was then quickly inserted into the hot zone of a horizontal furnace. All samples were treated at 530°C for 24 hours. Pre-sintering produced less than 1% densification. But after the pre-sintering the pellets were sturdy enough to be easily manipulated. SEM observations of the pre-sintered pellets show that particles near the surface began to neck while interior particles remained spherical. This difference is thought to reflect density gradients produced during compression. Figure 5 shows SEM micrographs of the surface of a pre-sintered pellet. The initial density of the sample was calculated by measuring its weight and volume. Calipers were used to measure the length and diameter of the pre-sintered pellet. The volume was then computed assuming a cylindrical shape. Because the indentations displace material but do not remove it, their presence does not significantly effect either the weight or the length of the sample.

3.3 Sintering

Sintering experiments were preformed in a horizontal furnace open to air. A schematic diagram of the experimental arrangement is shown in figure 6. In preparation for sintering experiments, the furnace profile was measured with the furnace control set at 600 ^{o}C, 700 ^{o}C and 800 ^{o}C. Figure 7 shows the profiles obtained with these settings. The profiles show that the gradients in a pellet that is offset 17cm from the furnace end can be reasonably approximated as linear over the 1.2cm length of a sample.

The pellets were suspended from the tips of two thermocouples which are inserted into the previously formed indentations; this arrangement provides intimate contact between thermocouple and sample, reducing error in temperature readings. This thermocouple placement is particularly important during gradient sintering when temperatures vary by 40°C/cm. A series of isothermal runs were made to determine a suitable combination of time and temperature for further study. The results are presented in figure 8. A time of 1 hour at 635°C was chosen for isothermal measurement because these conditions produced final densities near 1.9 g/cm^3 (75% of theoretical), about midway between initial density 1.6 g/cm^3 (62% of theoretical) and the density 2.3 g/cm^3 (90% of theoretical) at which continuous open pore channels between the particles are closed.

With the experimental conditions determined, several isothermal samples were made. The final density of isothermal samples was first obtained by measuring the final dimensions and weight. The radial shrinkage of isothermal samples is reported in table 3. While the radial shrinkage was fairly uniform, the axial shrinkage showed large scatter. This was due to primarily to a slight concavity present at each end of the sintered pellet. The concave curvature is in turn thought to reflect the sample geometry. To obtain

more accurate measurements of the density each sample was cut into 4-5 sections using a rotating diamond saw equipped with a micrometer. The two end sections were discarded, leaving 2-3 inner sections, each about 2 mm in length. The cutting produced sections with flush edges and uniform dimensions, making subsequent measurement with calipers more accurate. Table 1 lists the results of density measurements made on isothermal samples. Figure 9 shows the spread of densities in sections from the same isothermal sample. This figure shows that the three interior segments have a spread in density of 0.04 g/cc. Since the sections are taken from a single isothermal sample we attribute the spread to error produced during the sectioning and measurement. We will take this value as our error in density measurements. Note, in the estimation of error, the two end slices have been neglected because indentations were a large proportion of these sections, making accurate measurement of dimensions difficult. Although this figure is symmetric, with the center section most dense, other specimens showed more random variation. Density measurements were also made using a buoyancy technique. The results of these measurements were discarded because they showed more scatter than the caliper method.

Preparation of samples to be sintered in gradients was the same as that outlined for isothermal samples. By locating the sample near one end of the furnace, a steady state gradient of approximately 40°C/cm was produced. The sintering temperature was reached after approximately 5 minutes and did not drift significantly during the runs. The samples as they shrink appear to flow around the tip of the thermocouple, allowing the thermocouple position to remain fixed. This fixed configuration would account for the relative absence of thermal drift. After a run was completed, the linear gradient was used to calculate the position in the sample that experienced a local temperature

of 635 ^{o}C. Using the diamond saw, samples were sectioned so as to have an average temperature of 635 ^{o}C. Their densities were measured using calipers. The results are reported in table 2.

Sections of isothermal and gradient samples were later fractured so that the morphology could be observed. Scanning electron microscope (SEM) micrographs of the fracture surface are shown in figure 10 and figure 11.

3.4 Chemical Segregation

The model, represented by equation (4), which predicts that temperature gradients provide an increased driving force for densification, assumes a homogeneous material. However, temperature gradients are known to drive chemical de-mixing. DeJonghe and Rahamen[17] found that temperature gradients produced significant de-mixing for Y-Ba-Cu-O superconductors. To determine whether the model is strictly applicable to these experiments it is necessary to investigate the chemical homogeneity of the sintered pellets. For glass, the problem of chemical de-mixing would be particularly acute. Since the viscosity of glass is strongly dependent on composition, a local variation in composition would lead to locally variable viscosity. In such a system it would be pointless to speculate whether an observed increase in density was due to temperature gradients or simply the result of lower viscosity.

EDX analysis was used to study the chemical composition as a function of position in gradient and isothermal samples. An isothermal sample sintered at 635°C for 1 hour was fractured, mounted and carbon coated. Exterior and fracture surfaces were examined at the center and at each end. The results, contained in table 5 show the composition measured in each section. Again we have calculated the averages, standard deviation, and reliability for each component.

The exterior of a gradient sample was examined for chemical homogeneity. To accentuate the possible effects of chemical segregation this sample was allowed to sinter for three hours in the standard gradient (620°C - 660°C). Starting at the cold end of the sample, section 1, composition measurements were made at intervals of approximately 1 mm. The results are contained in table 6. The data for Sodium are plotted in figure 12.

4 DISCUSSION

4.1 Density Measurement

The theory developed by Searcy predicts that a driving force for enhanced densification is provided by temperature gradients regardless of the mechanism of transport. Temperature gradients have been shown to cause increased rate of groove smoothing in surfaces of Al_2O_3 and an increased rate of densification in MgO compacts. Since both Al_2O_3 and MgO are crystalline, one can ask whether or not the effect depends upon a mechanism that was particular to crystalline bodies. It was thus of interest to investigate the effect of temperature gradients on the densification of glass powders, since they are known to densify by viscous flow.

To determine whether temperature gradients were responsible for increased densification it was necessary to compare samples heated in gradients to isothermal samples. In the ideal isothermal experiment a sample would sinter for a time interval t at temperature T. In practice, however, there are undesired end effects. Unless the sintering can be delayed until a catalyst is introduced, some sintering will occur during heating and cooling. The heating period is particularly important because the high initial surface areas provide a large driving force for densification. Further complexities are present if one recognizes that the finite size and thermal conductivity of a sample will necessarily produce a transient temperature gradient from the core to the outer surface of the sample. Thus, nominally isothermal samples have complexities due to the transients produced during heating and cooling.

These complications are somewhat mirrored in the gradient samples since these also must be heated to the desired steady state conditions. Samples inserted into a static gradient will experience transient gradients along the radial direction, as well as the desired axial gradient. The transient radial gradient in the section at 635°C, the temperature of interest, should be nearly the same as for the isothermal case. It is reasonable to assume that the densification produced during the transient stage is the same for both samples, so that the transient periods reduce the time period fo the comparison experiment. That is, rather than comparing samples that were sintered differently for 1 hr we are comparing samples sintered 10 minutes under similar transient conditions followed by 50 minutes at the desired differing conditions. But it must be recognized that although most of the time is spent at well characterized conditions, the time spent coming to the steady state may be disproportionately significant, because the initial effects, when the driving force is highest, are obscured.

Another complication that is relevant to studies conducted in temperature gradients is a net mass flux relative to the laboratory reference provided by the fixed position of the thermocouple tips. Petusky and Bowen[18] observed a temperature gradient driven mass flux in an iron-aluminium spinel wafer. It appeared that cations diffused through the lattice and combined with oxygen at the cold interface, causing translational movement of the wafer in that direction relative to the laboratory frame. We did not anticipate significant mass translation flux and therefore made no provision for its measurement. After sintering, samples were examined for evidence of mass flux. Gradient and isothermal samples appeared the same. Both types of samples showed a slight concave curvature at each end. This is thought to reflect sample geometry.

The results of the density measurements are contained in tables 1 and table 2. The average increase in density for the section of the gradient samples at 635°C was 0.368 g/cm^3 and 0.332 g/cm^3 for isothermal samples. As expected, the increase in density was greater for samples heated in the static gradient. However, referring again to figure 8 we see that there is a 0.04 g/cm^3 uncertainty produced during measurement. Thus the 0.03 g/cm^3 difference in density produced by the differing heat treatments provides only weak support for the theory which predicts increased densification.

Figures 10-11 show SEM micrographs of fracture surfaces of isothermal and gradient sections. The micrographs show that the spheres have begun to sinter yet retain their basic spherical shape and size. As one would expect from the density measurements, there is no clearly distinguishable difference in the degree of sintering.

4.2 Chemical Segregation

Chemical analysis was obtained using EDX in the SEM. This type of chemical analysis sacrifices energy resolution to obtain spatial resolution. As a result, EDX is usually accurate to within about 1 weight percent. Although spatial resolution makes this technique less accurate than other techniques, it gives one the ability to obtain local measurements. By obtaining a series of measurements one may construct a composition profile or map.

The results of our EDX composition measurements are given in table 4, table 5, and table 6. The last row of each of these tables lists the standard deviation as a fraction of the average value. By normalizing the standard deviation in this manner we are able to compare the scatter in measurements for each of the components. We find that Na, Si, and K provide the most stable readings, and thus we choose to focus our analysis in terms of these components. There are two interesting phenomenon occurring in terms of these species. The Na appears to remain relatively homogeneous during isothermal heating (table 2). However, in the gradient, Na segregates to the hot end of the sample (figure 12). This result, similar to DeJonghe's, is the sort of segregation that we anticipated might be driven by a temperature gradient. We note that the segregation found for Na is not mirrored by the other constituents. This may reflect a higher mobility for Na which is the smallest cation for which we have data. Kingery et al.[19] report that monovalent cations diffuse more rapidly at a given temperature than divalent cations. Thus, it is reasonable that Na might display more clearly a segregation that was slower to develop for the other species.

Si and K show an interesting and quite different sort of segregation. When heated, either isothermally or in a gradient, Si segregates to the interior while K segregates to the surface. The data are most convincing for Si heated isothermally. The data values obtained from the fracture surface are significantly higher than the exterior values. This result is supported by the data obtained from the surface of our gradient sample. The values from the gradient samples surface are consistently lower than the average value of the starting material.

5 CONCLUSION

The densification of glass powder compacts was measured for samples fired both isothermally and in gradients of 40°C/cm. Samples were compared on the basis of the densification produced by 1 hour at 635°C. Samples were prepared using sodium-silicate glass particles which were spherical and ranged in size (30 μm-65 μm).

The isothermal samples experienced an average increase in density of 0.33 g/cm^3 while gradient samples averaged a slightly higher increase of 0.38 g/cm^3. Although the results produced are in accord with the proposed theory, the magnitude of the increase is insufficient to provide clear evidence that the gradient is responsible for increased densification.

To observe the expected increase in densification, it may be necessary to employ an amorphous system that can be catalyzed to begin sintering after steady state conditions have been established. However, lacking such a system, one can only attempt to accentuate gradient effects. Since increasing the scale of the system will reduce the effects of surface curvature, one might observe the growth of necks between contacting spheres and compare the results produced by gradient and isothermal conditions. In this way one could avoid the limitation to size imposed by the problems of mechanical stability in compacts of large spheres.

6 TABLES

TABLE 1
Isothermal Density Measurements

Density Measurements for Samples Heated at 635 ^{o}C

sample #	initial density	final density	density change
	(g/cm^3)	(g/cm^3)	(g/cm^3)
I1	1.57	1.91	.34
I1	1.57	1.92	.35
I1	1.57	1.88	.31
I2	1.63	1.93	.30
I2	1.63	1.91	.28
I3	1.59	1.88	.29
I3	1.59	1.93	.34
I3	1.59	1.89	.30
I4	1.58	1.90	.32
I4	1.58	1.93	.35
I5	1.57	1.96	.39
I5	1.57	1.94	.37
I5	1.57	1.95	.38
avg			.33

Table 2
Gradient Density Measurements

Density at 635 ^{o}C of Samples Held in a Gradient of 40 $^{o}C/cm$

sample #	initial density	final density	density change
	(g/cm^3)	(g/cm^3)	(g/cm^3)
G1	1.53	1.86	.33
G2	1.55	1.95	.40
G3	1.57	1.96	.39
G4	1.60	1.96	.36
G5	1.61	1.97	.36
G6	1.60	2.02	.42
avg			.38

Table 3
Axial (ΔD) Shrinkage
of Isothermal and Gradient Specimens

sample #	ΔD	$\Delta D/D_0$
I1	.055	.065
I2	.050	.059
I3	.050	.059
I4	.050	.059
I5	.060	.071
G1	.050	.059
G2	.060	.071
G3	.060	.071
G4	.060	.071
G5	.060	.071
G6	.065	.076

Table 4
Initial Glass Composition

wt. %	B_2O_3	Na_2O	MgO	Al_2O_3	SiO_2	K_2O	CaO	BaO
reported	2	10	1	1	67	7	5	6
measured	--	16.98	1.43	1.92	66.32	4.82	4.16	4.37
measured	--	16.98	1.32	1.44	66.21	4.65	3.94	5.45
measured	--	15.10	1.37	2.01	65.66	5.02	4.29	6.54
average	--	16.35	1.37	1.79	66.06	4.83	4.13	5.45
deviation	--	1.08	0.06	0.31	0.35	0.19	0.18	1.08
avg./dev.	--	0.07	0.04	0.17	0.01	0.04	0.04	0.20

Table 5
Isothermal Composition Profile
After Heating at 635 ^{0}C for 1 Hour

	Na_2O	MgO	Al_2O_3	SiO_2	K_2O	CaO	BaO
frac 1	17.73	1.54	1.54	65.63	5.48	3.31	4.86
frac 2	16.96	1.87	2.38	66.07	5.45	2.82	4.45
frac 3	14.62	1.39	2.07	67.08	5.48	3.69	5.67
ext 1	16.32	1.54	1.49	64.97	5.76	3.95	5.98
ext 2	17.61	2.08	2.08	62.96	5.38	3.30	6.60
ext 3	16.90	2.81	1.35	64.92	5.89	3.05	6.35
average	16.56	1.66	1.82	65.27	5.57	3.35	5.65
deviation	1.14	0.26	0.41	1.39	0.20	0.41	0.84
avg./dev.	0.07	0.16	0.23	0.02	0.04	0.12	0.15

Table 6
Gradient Composition Profile
After Heating Between 620 °C and 660 °C
for 3 Hours

	Na_2O	MgO	Al_2O_3	SiO_2	K_2O	CaO	BaO
1	14.63	0.83	1.12	60.85	8.04	3.20	11.33
2	15.69	1.25	1.76	58.35	8.67	4.35	10.50
3	17.14	1.07	1.61	57.83	8.80	4.99	8.56
4	16.72	2.18	1.82	58.65	8.99	3.93	7.71
5	16.61	1.84	2.57	56.95	8.60	5.08	8.35
6	16.45	1.96	2.17	56.19	8.60	6.28	8.35
7	16.54	1.37	1.86	56.71	9.41	5.27	8.84
8	17.17	1.21	1.57	57.74	8.71	3.47	10.13
9	19.25	2.74	2.22	56.08	8.00	2.96	8.76
10	20.99	1.01	2.16	55.24	8.33	4.72	7.55
average	17.12	1.55	1.88	57.46	8.61	4.43	9.01
deviation	1.79	0.61	0.41	1.60	0.42	1.04	1.24
dev./avg.	0.10	0.39	0.22	0.03	0.05	0.24	0.14

7 FIGURES

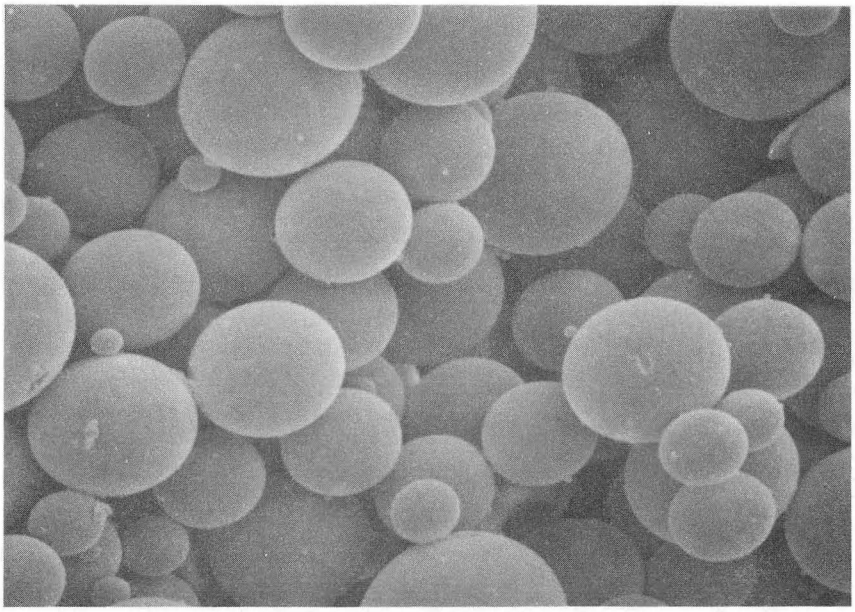

(a) —— 27.0 μm

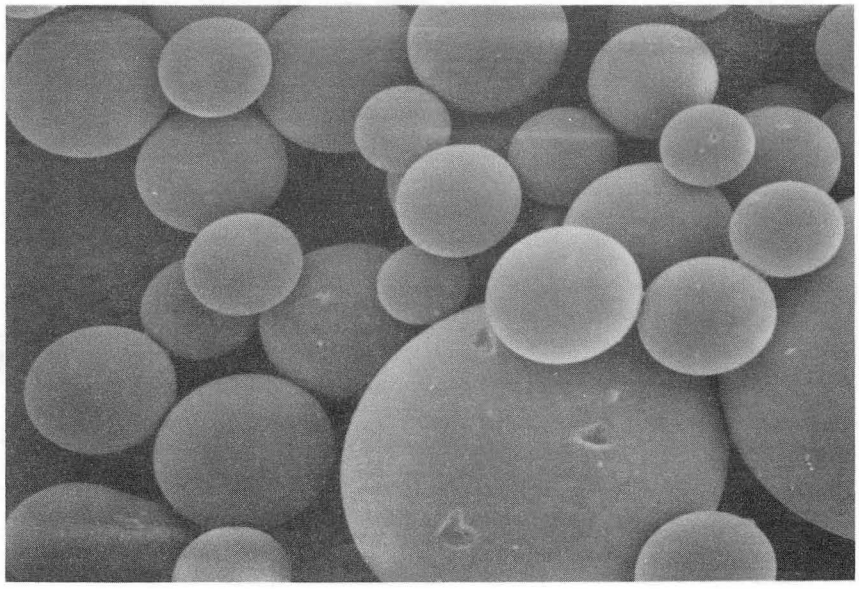

(b) —— 27.0 μm

XBB 900-9660

Figure 1: Starting Material. Glass powder obtained from the Jaygo Co.

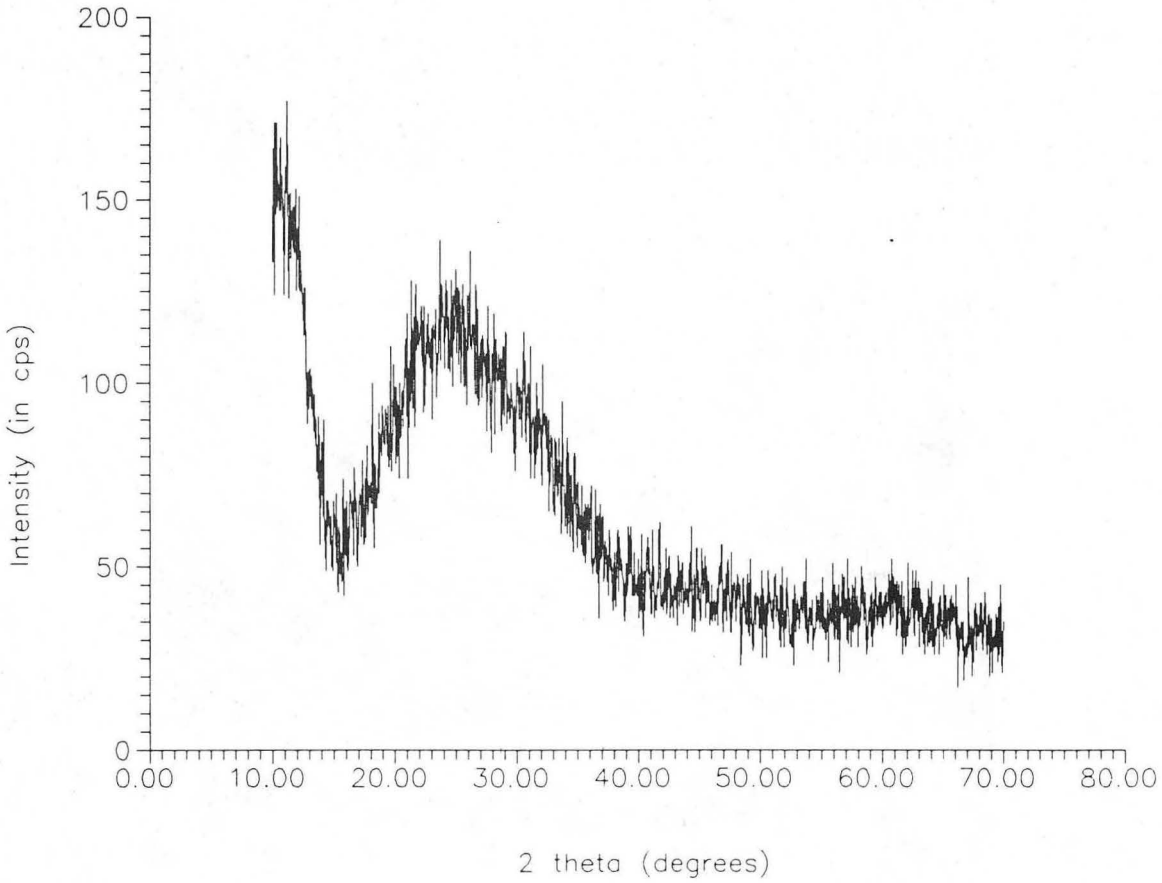

XBL 9011-3819

Figure 2: X-ray diffraction pattern of starting material.
The pattern is characteristic of amorphous materials.

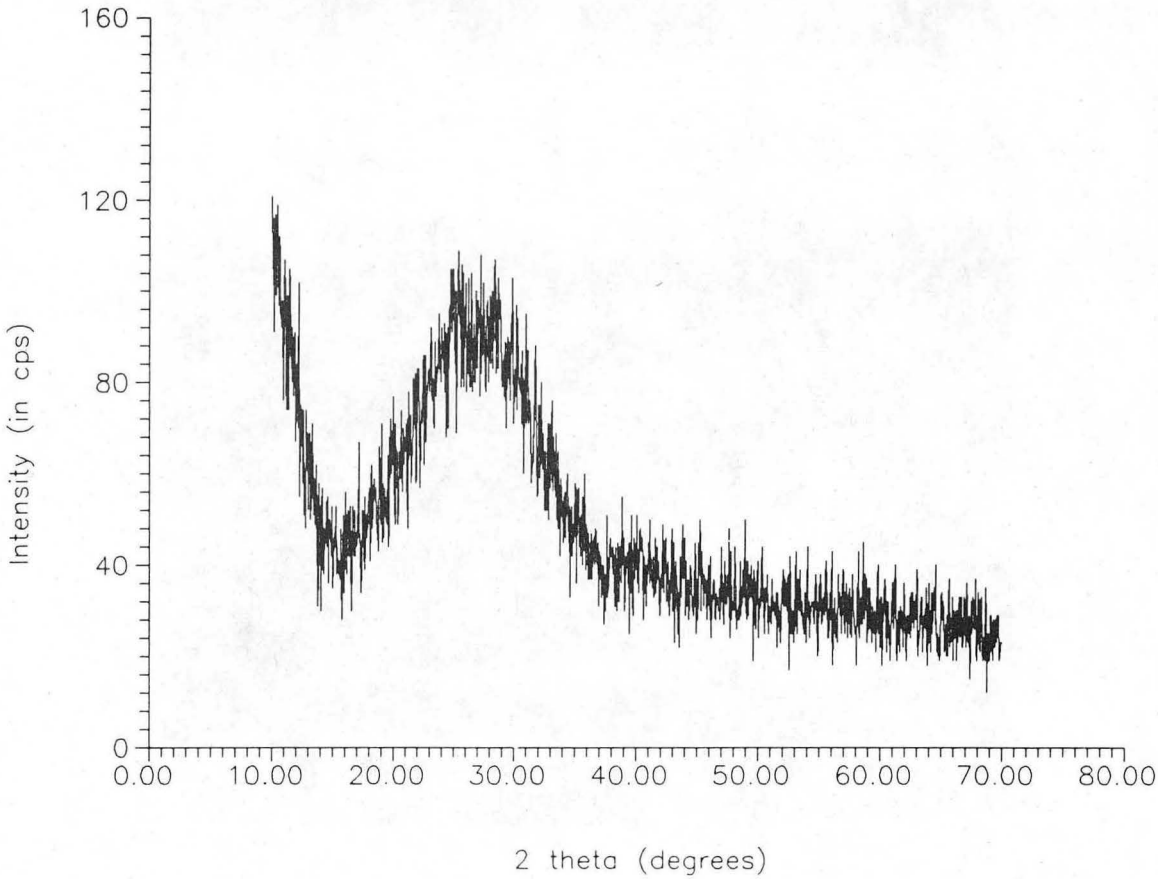

XBL 9011-3820

Figure 3: X-ray diffraction pattern of powder that was heated at 700 ^{o}C for 24 hours then ground to pass through a #200 mesh screen.

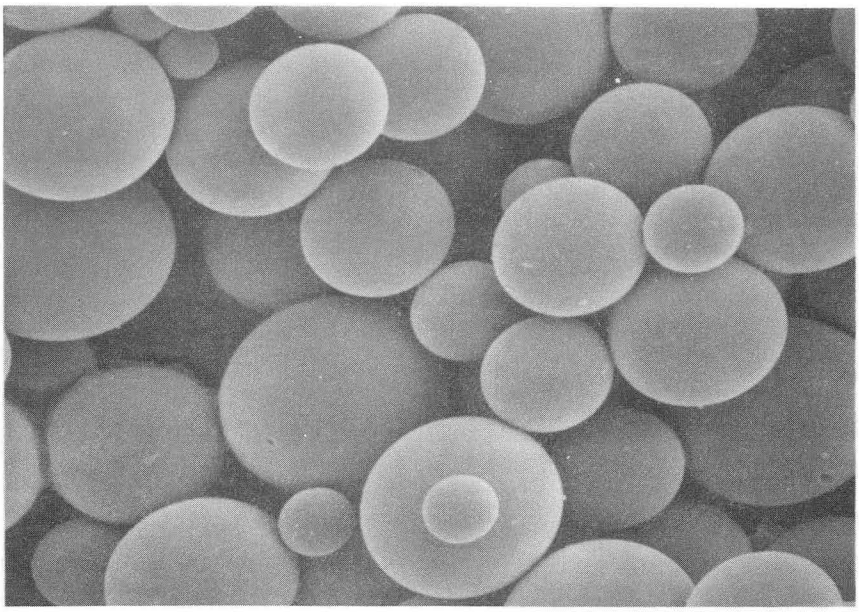

(a) —— 27.0 μm

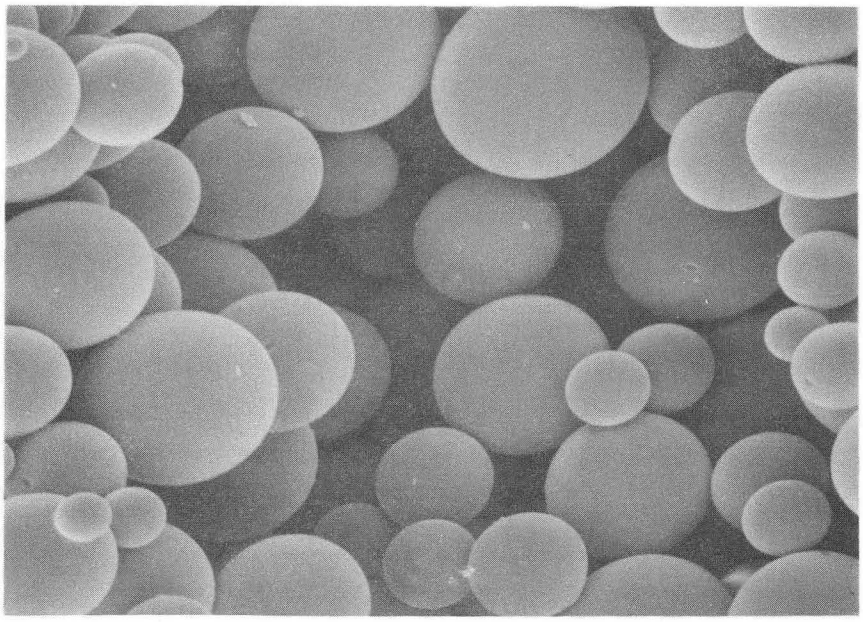

(b) —— 27.0 μm

XBB 900-9961

Figure 4: Classified Material. Glass powder collected between #200 and #325 mesh screens.

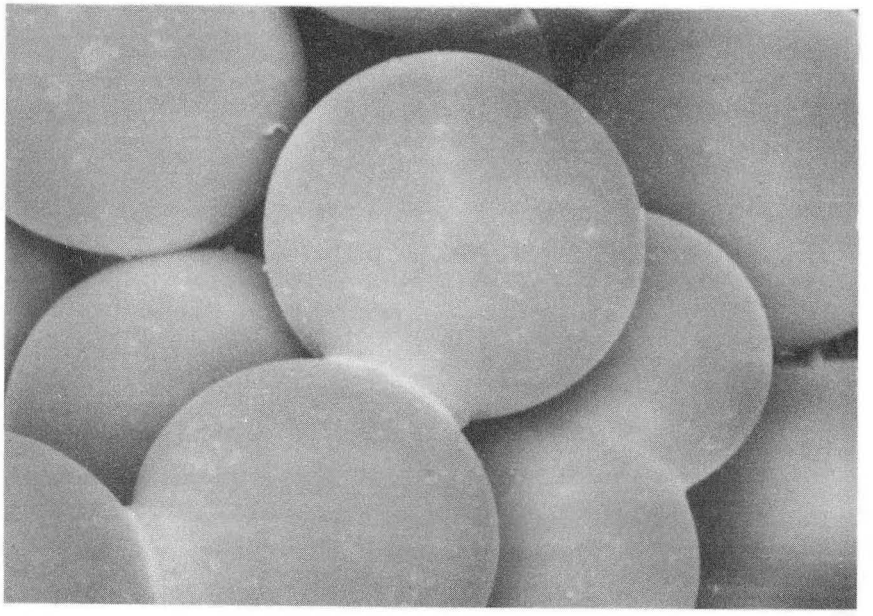

(a) —— 11.0 μm

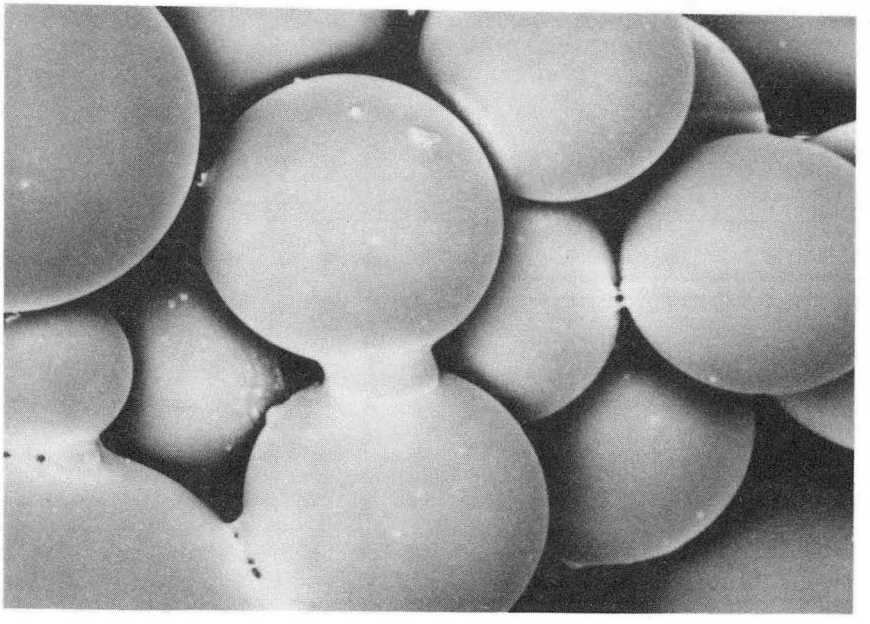

(b) —— 8.9 μm

XBB 900-9962

Figure 5: Surface of pre-sintered pellet showing neck formation.

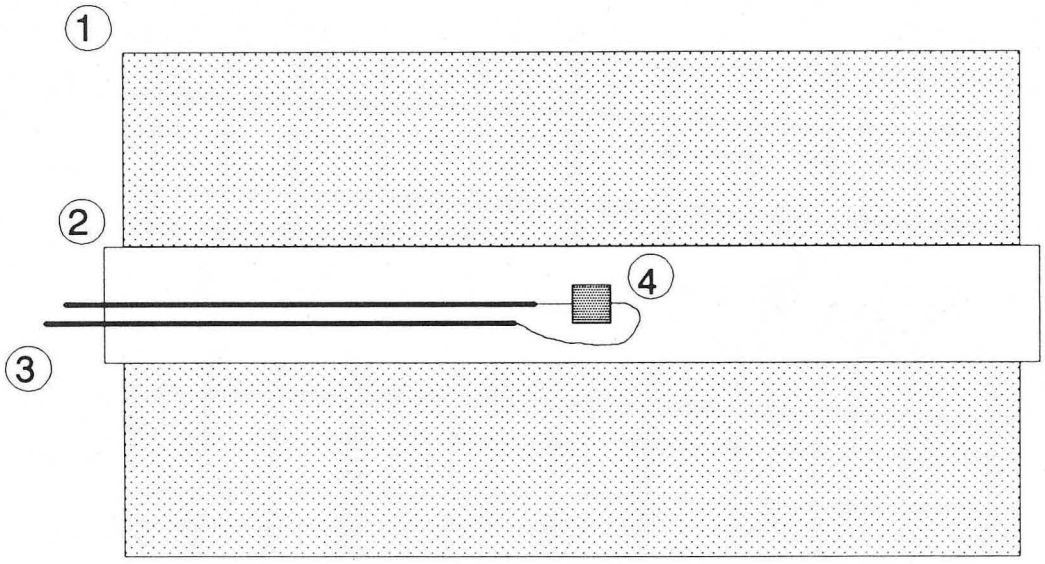

XBL 9011-3821

Figure 6: Schematic Diagram of Experimental Equipment.

1. Furnace
2. Alumina Tube
3. Chromel-Alumel Thermocouple
4. Sample Pellet

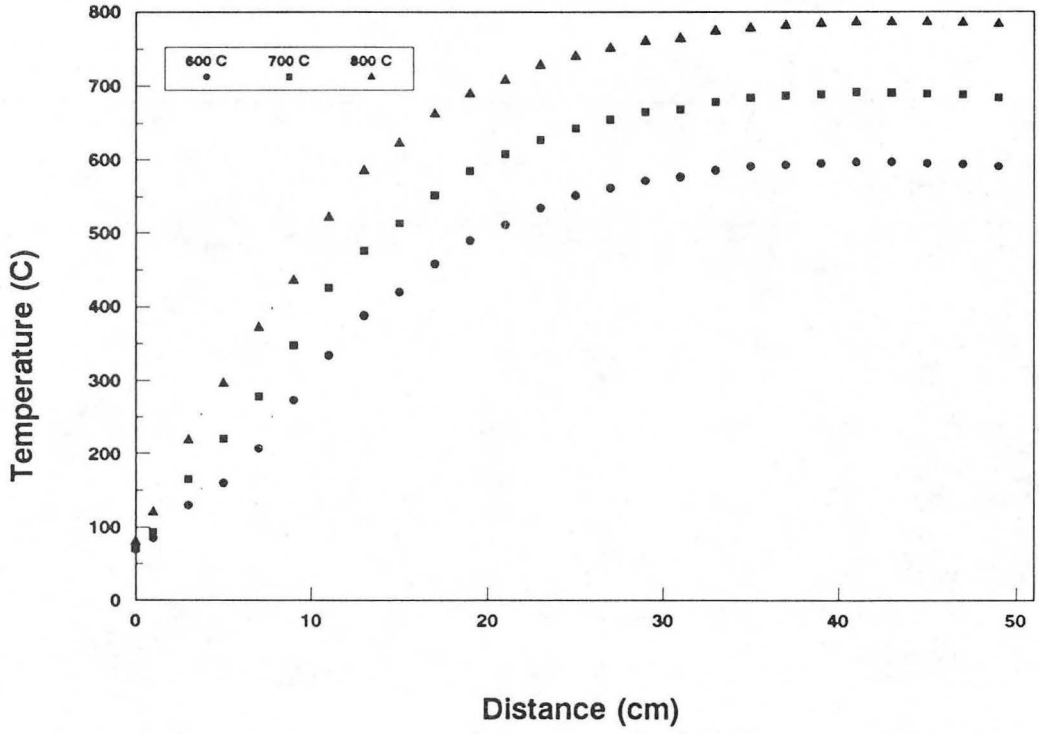

XBL 9011-3822

Figure 7: Furnace Profiles for Temperature Control Set at 600°C, 700°C and 800°C.

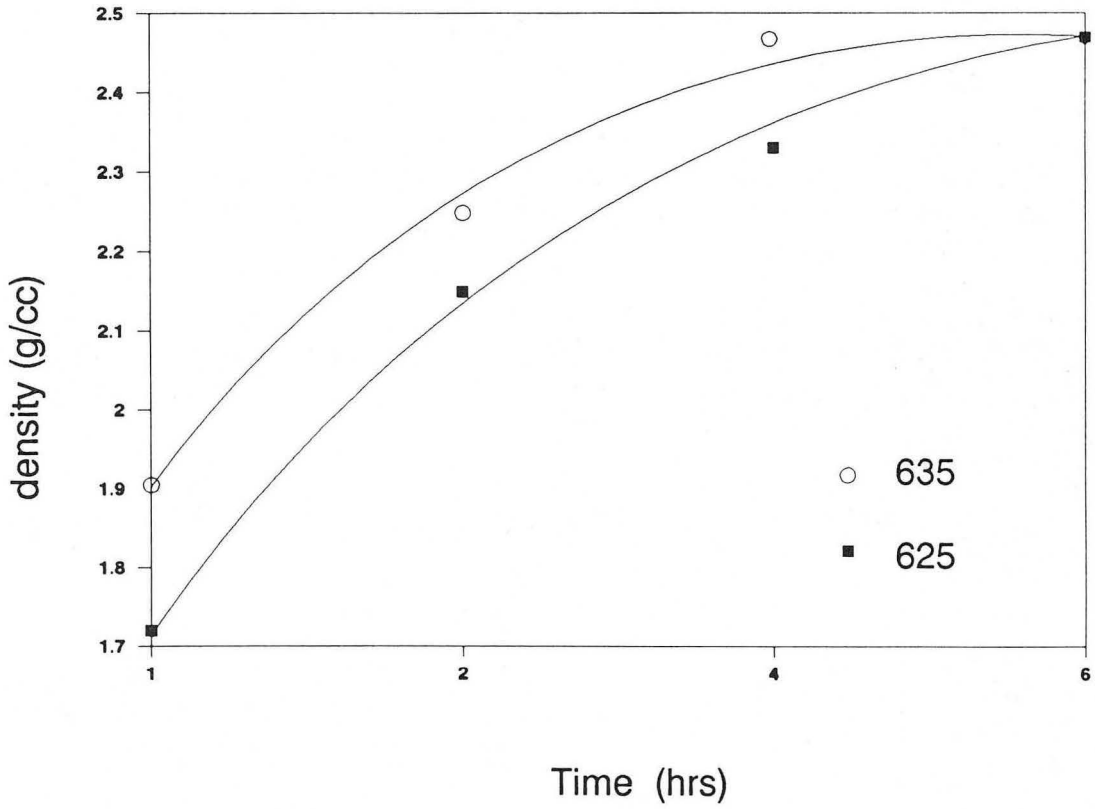

XBL 9011-3823

Figure 8: Density as a Function of Time for Samples Heated Isothermally.

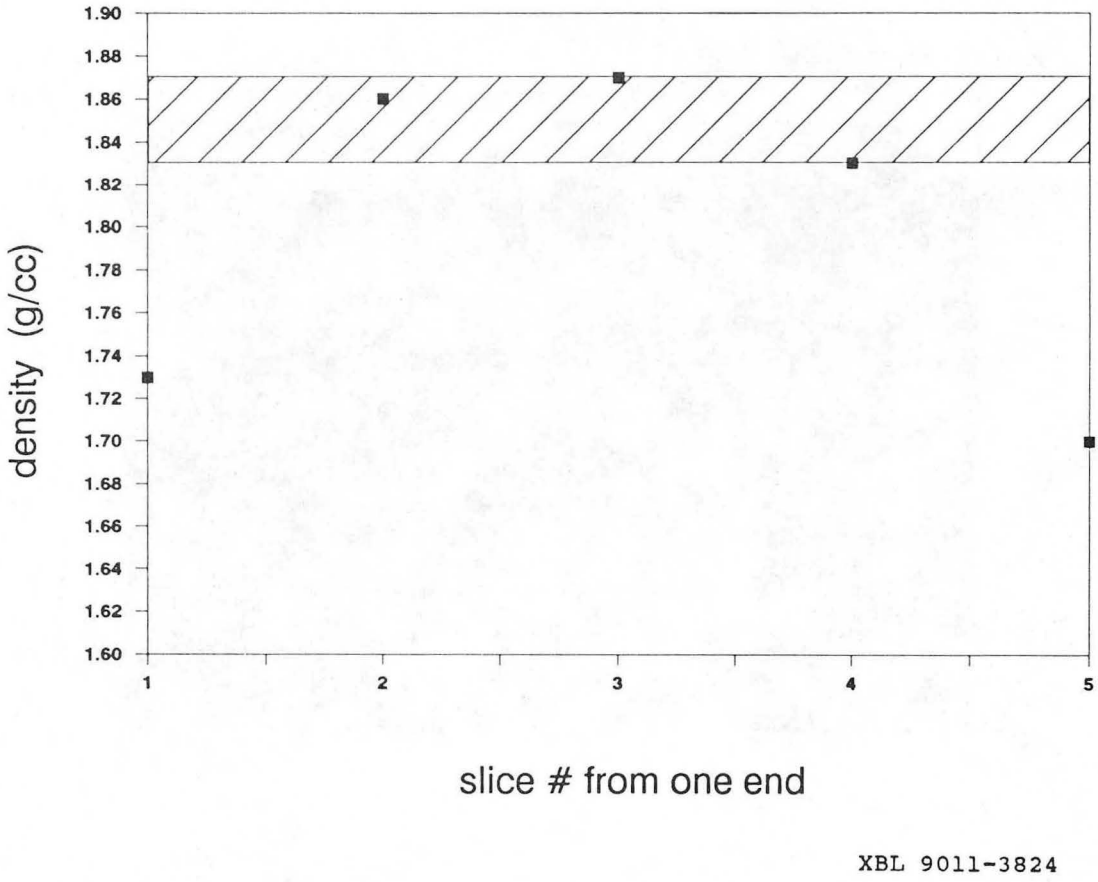

Figure 9: Variation in Density of Slices from and Isothermal Sample.

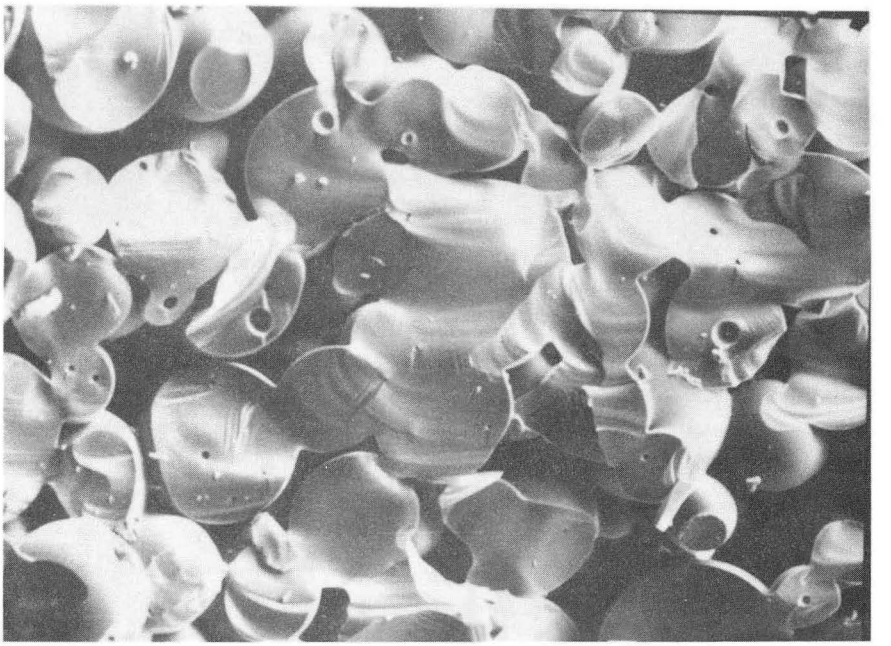

(a) —— 25.0 μm

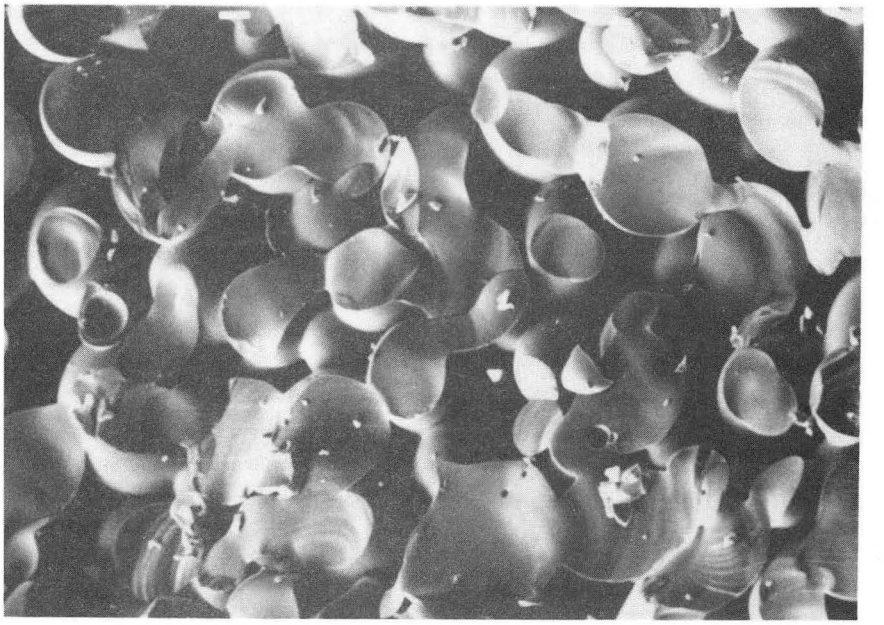

(b) —— 25.0 μm XBB 900-9963

Figure 10: SEM Micrographs of fracture surfaces of isothermal samples.

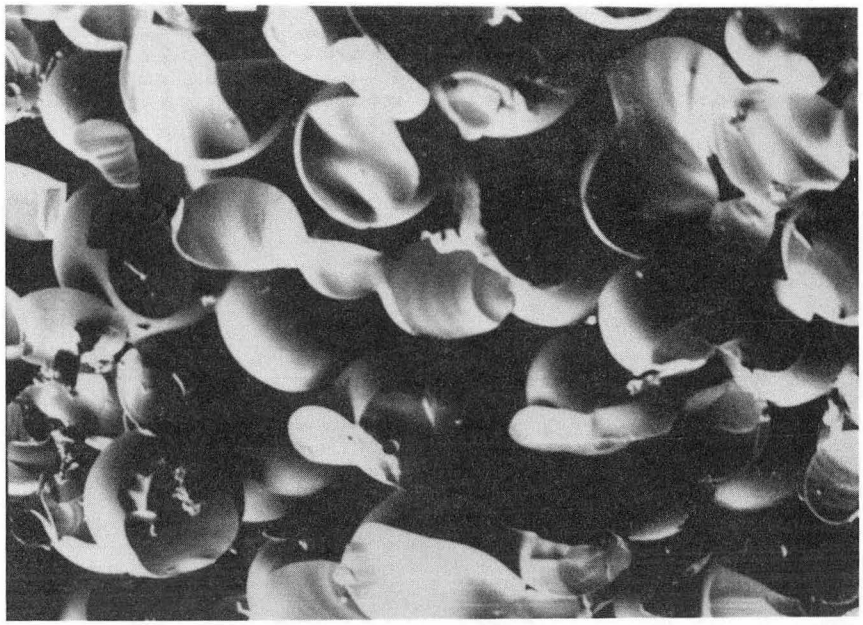

(a) —— 25.0 μm

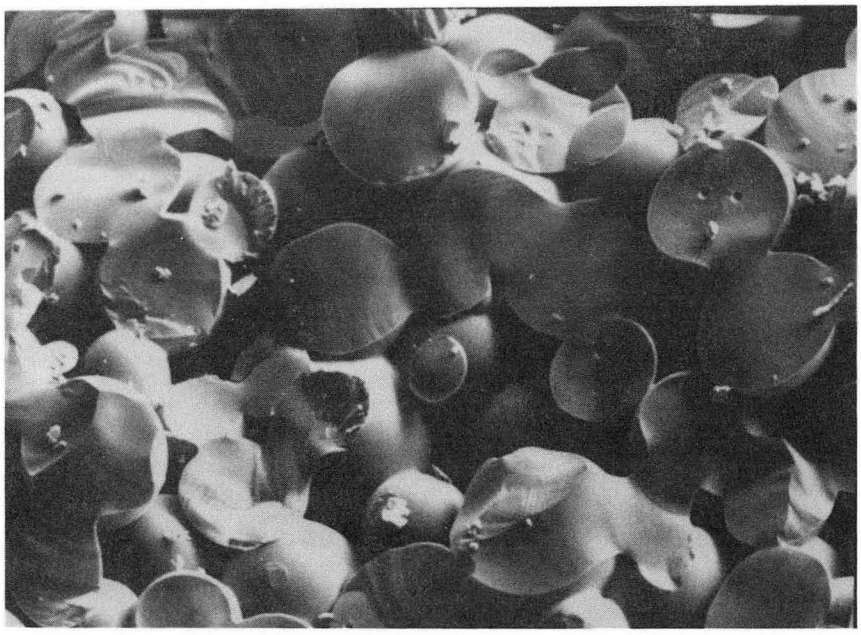

(b) —— 25.0 μm

XBB 900-9964

Figure 11: SEM Micrographs of fracture surfaces of gradient samples.

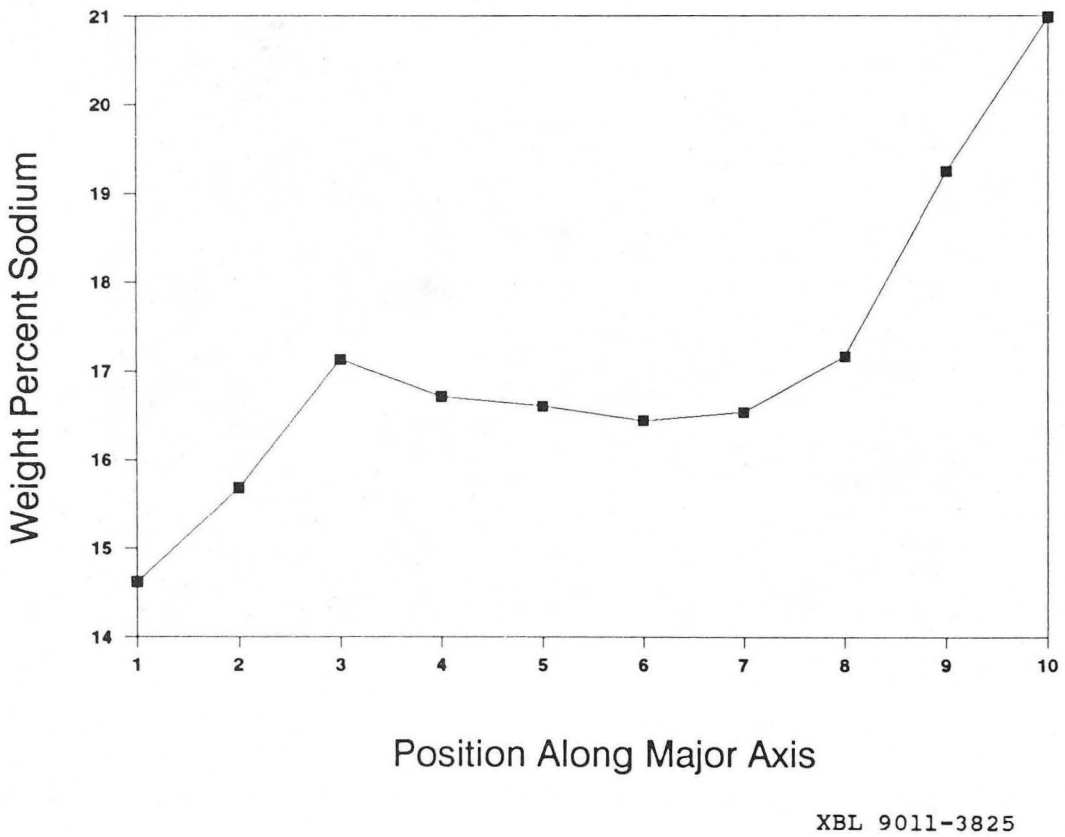

Figure 12: Weight Percent of Na2O as a Function of Position Along the Major Axis in a Gradient Specimen.

LAWRENCE BERKELEY LABORATORY
CENTER FOR ADVANCED MATERIALS
1 CYCLOTRON ROAD
BERKELEY, CALIFORNIA 94720